AIP Conference Proceedings

Leak Location in Plates: Compensation for MultiMode dispersion

M. Strei, R. Roberts, S. Holland, and D. E. Chimenti

Citation: AIP Conf. Proc. **700**, 1398 (2004); doi: 10.1063/1.1711779
View online: http://dx.doi.org/10.1063/1.1711779
View Table of Contents: http://proceedings.aip.org/dbt/dbt.jsp?KEY=APCPCS&Volume=700&Issue=1
Published by the American Institute of Physics.

LEAK LOCATION IN PLATES: COMPENSATION FOR MULTI-MODE DISPERSION

M. Strei, R. Roberts, S. Holland, and D. E. Chimenti
Center for NDE and Aerospace Eng Dept, Iowa State Univ, Ames IA 50011

ABSTRACT. The problem of noise source location in a plate-like structure using time of flight data recorded at sparsely distributed measurement locations is examined. The cross-correlation approach to source triangulation is not generally applicable to signals carried by multiple dispersive plate wave modes. This work examines the extensions to the principles of cross-correlation-based triangulation needed to robustly determine source location.

INTRODUCTION

This paper addresses the location of a leak in a structure which is generating sufficient structure borne noise so as to be detected by remotely positioned sensors. It is desired to compare the relative transit times to three bracketing sensors, to "triangulate" the source location. Such an approach assumes that there are unique transit times associated with the received signals, which can be determined by noting the peak location in the cross-correlation of signal pairs between the three receivers. The problem addressed in this work arises from the fact that signals transported by plate waves do not do not necessarily satisfy these underlying assumptions. Specifically, plate-like structures transmit energy in multiple modes of wave propagation, and the velocity of propagation for each mode depends on the spectral features of the signal. Consequently, a single event generated by the source will be received as multiple events by the receivers. Furthermore, the temporal shape of the signal carried by each wave mode will vary with distance, so that signals propagating different distances can not effectively be compared via cross correlation to determine arrival time differences. The net effect of these phenomena, when cross-correlation based triangulation is attempted, can be the generation of false source indications. If not properly compensated for, this fundamental inadequacy in signal processing can lead to an unacceptably high variability in the accuracy of acoustic emission leak location.

Previous work examined means to compensate for effects of multiple mode dispersive propagation, for the problem of noise source location in liquid transport pipelines.[1,2] That work demonstrated how the effects of multi-mode dispersion can foil cross-correlation based source location analysis, and how, through analysis of measured signals in both spatial and temporal frequency domains, the ill-effects of multi-mode dispersion can be removed. The problem in that work was viewed as essentially one dimensional. In the work presented here, the concepts explored in the one-dimensional pipeline problem are applied to the two dimensional problem of source location in plate-like structures. Specifically, the NASA application motivating this work is the detection of air leaks in the outer skin of the International Space Station.

CP700, *Review of Quantitative Nondestructive Evaluation Vol. 23,* ed. by D. O. Thompson and D. E. Chimenti

BACKGROUND

An example calculation is presented which demonstrates the problem introduced by multi-mode dispersion. A measurement configuration using a 1mm thick plate is assumed as depicted in Fig.(1). Sensors are positioned at two locations denoted "A" and "B", which bracket the source location. The signal generated by the source propagates as a sum of plate modes to the sensors. The sensors also detect reflections of the signals from the edge of the structure. The signals detected by the sensors are compared in Fig.(2). To depict the impact of multi-mode dispersion, this example assumes the source generates a broadband impulse shown in Fig.(2a). If the signal were transmitted by a single non-dispersive mode of propagation, the signal detected by the sensors would be time-delayed replicas of the signal generated by the source. It is assumed here, however, that the signal is carried by the three lowest order plate modes, in the bandwidth of 400 to 3600 kHz. The effects of multi-mode dispersion is seen in the signals detected at sensor positions "A" and "B", shown in Figs.(2b,c). The temporal shapes of the signals are seen to be substantially different. The effect of this difference is seen in the cross-correlation shown in Fig.(3). Rather than displaying a single peak at the difference in transit time to the two sensors, the result shows a broad distribution of fictitious source locations. For a leak, the received signals would be the convolution of the signals in Fig.(2) with the leak-generated random noise. In this case, Fig.(3) represents either the limit of averaging many cross-correlated finite length noise segments, or the limit for a single noise segment approaching infinite length.

The detected signals in Fig.(2) propagate as a sum of wave modes, each propagating with a different frequency dependent wave number k(ω). For a source in an unbounded plate, the signal at sensor A is expressed in the temporal frequency domain as

$$v^A(s^A, \omega) = N(\omega) \sum_n A_n(\omega) \exp(i k^n(\omega) s^A) \tag{1}$$

where N(ω) is the temporal frequency response of the source, $A_n(\omega)$ is the amplitude of the coupling of source and sensor into mode type n, and s^A is the distance between source and sensor. Consider the windowed Fourier transform of eq.(1) in distance s, over the spatial extent of a window function W(s) positioned at s^A

$$\hat{v}^A(\gamma, \omega) = \int W(s)\, v^A(s^A + s, \omega) \exp(-i \gamma s)\, ds \tag{2}$$

Using eq.(1), it is seen

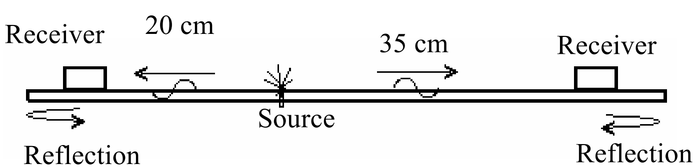

FIGURE 1. Measurement configuration modeled in the signals presented in Fig.(2).

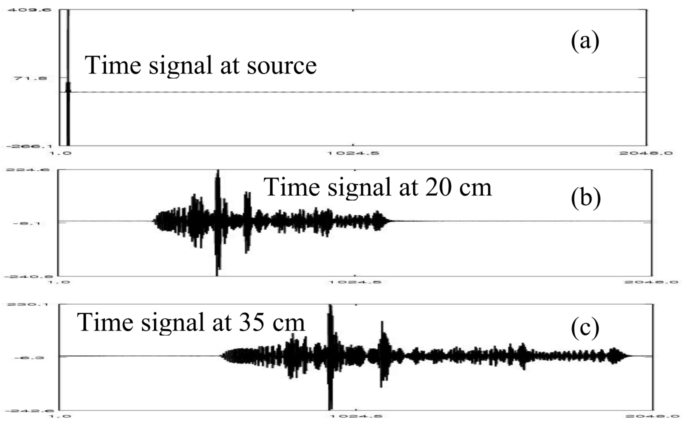

FIGURE 2. Signals computed for configuration of Fig.(1).

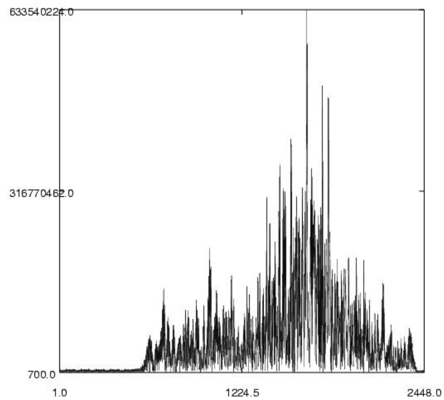

FIGURE 3. Cross-correlation of signals (b), (c) in Fig.(2).

$$\widehat{v}^{A}(\gamma,\omega) = N(\omega) \sum_{n} A_{n}(\omega)\, \hat{W}(\gamma - k^{n}(\omega)) \exp(i\, k^{n}(\omega)\, s^{A}) \tag{3}$$

Assuming that each wave mode has a distinct wave number at a particular frequency, a window can always be defined such that, for sufficient window length

$$\hat{W}(k^{n}(\omega) - k^{m}(\omega)) \cong \delta_{nm} \tag{4}$$

leading to

$$\widehat{v}^{A}(k^{n}(\omega),\omega) \cong N(\omega)\, A_{n}(\omega) \exp(i\, k^{n}(\omega)\, s^{A}) \tag{5}$$

Eq.(5) indicates how, through Fourier transformation in time and space, the components of the received signal carried by different modes of propagation can be isolated.

Using mode-isolated signals as indicated by eq.(5), the concept of cross-correlation can be generalized for application to multi-mode dispersed signals. Assuming mode isolated signals are available from positions A and B for a particular mode m, the difference in propagation distances can be determined by noting value of Δs yielding the peak in the expression

$$G(\Delta s) = \int \hat{v}^{A}(k^{m}(\omega),\omega)\, \hat{v}^{B*}(k^{m}(\omega),\omega)\, \exp(-i\, k^{m}(\omega)\, \Delta s)\, d\omega \qquad (6)$$

Note that evaluation of eq.(6) assumes the dispersion relation $k^{m}(\omega)$ is known for the particular mode examined. This information is readily discerned by examining the energy distribution of the measured signals in the temporal-spatial frequency plane.
Also note that, for the case of no dispersion, $k^{m}(\omega) = \omega / c_m$, where wave velocity c_m is independent of frequency, hence eq.(6) reduces to the familiar expression for cross-correlation of two signals. Eq.(6) is therefore referred to as a generalized cross-correlation, generalized for application to signals undergoing dispersion.

The data processing described above is applied to the model signal predictions shown in Fig.(2b,c). Signals are obtained at a grid of 16 points with 0.5 mm spacing at measurement positions A and B. Fast Fourier Transforms are then applied in both time and space. The temporal-spatial frequency spectra amplitude of one of the signals is displayed in Fig.(4). It is seen that the signal energy is distributed along the mode dispersion curves $k^{n}(\omega)$, for three modes. It is also seen that energy is also contained in the negative spatial frequencies, corresponding to reflections from the edge of the plate, that is, signals propagating toward the source, rather than away from it. The number and spacing of the data points are determined by considering familiar signal sampling criteria in connection with Fig.(4). It is evident that the number and spacing of the spatial measurement points must be sufficient to cover the entire spatial frequency bandwidth of the signal, and to allow resolution (i.e. separation) of the propagating wave modes. Fig.(5) shows the evaluation of Eq.(6) using the lowest order mode of the two signals, indicated as mode 1 in Fig.(4). It is seen that the source location is unambiguously identified by an isolated peak.

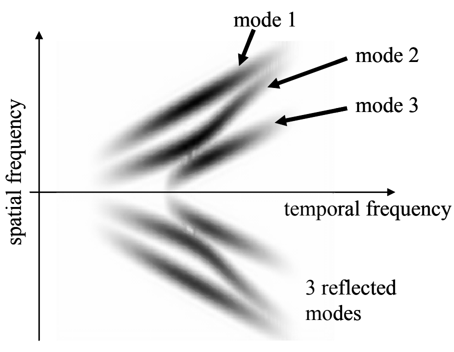

FIGURE 4. Space-time spectra of signal.

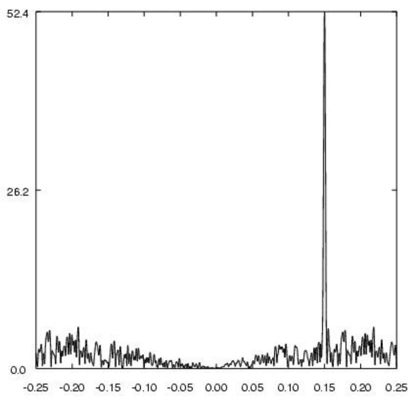

FIGURE 5. Generalized cross-correlation of signals.

IMPLEMENTATION USING CROSS-CORRELATION PAIRS

The computation shown in Figs.(1-5) demonstrates how the ill-effects of multi-mode dispersion on time-of-flight source triangulation can be compensated for by spatial Fourier transformation of measured signals. It is noted, however, that, when considering the analysis of a non-repeating noise signal, spatial Fourier transformation of the signal requires simultaneous capture of the signal at all array positions as the signal passes. In the above example, this would require 16 digitizers interfaced to a 16 element array at each measurement location. This is not outside the scope of current technology. However, it was observed that an alternative approach to data collection is available to obtain an equivalent result, using simpler instrumentation. Specifically, it is noted that the product of signal spectra under the integrand in Eq.(6) could alternately be obtained by Fourier transforming the cross-correlation of signals measured at positions s^A and s^B. This approach is discussed explicitly for the case of a random noise source.

Consider the mean of the cross-correlation of signals obtained at measurements positions s^A and s^B, denoted in the temporal frequency domain as

$$< C(s^A, s^B, \omega) > = < v^A(s^A, \omega)\, v^{B*}(s^B, \omega) > \tag{7}$$

Using eq.(1), it is seen

$$< C(s^A, s^B, \omega) > = P(\omega) \sum_n A_n(\omega) \exp(i\, k^n(\omega)\, s^A) \sum_m A_m^*(\omega) \exp(-i\, k^m(\omega)\, s^B) \tag{8}$$

where $P(\omega)$ is the mean power spectrum of the noise source

$$P(\omega) = < N(\omega)\, N^*(\omega) > \tag{9}$$

The mean power spectrum of a random noise source will generally be a function having an impulse-like Fourier transform, enabling a sharply defined location peak in the source location algorithm. The mean of the cross-correlated signals is spatially Fourier transformed in s^A and s^B, as indicated in eq.(2), using a window function displaying the property of eq.(4). The resulting spectrum $\hat{C}(\gamma^A, \gamma^B, \omega)$ is a function of temporal frequency ω and two spatial frequency variables γ^A, γ^B, corresponding to spatial variables s^A, s^B. The contribution of a single isolated wave mode m is examined by evaluating this three-dimensional spectrum over the curve

$$\gamma^A = \gamma^B = k^m(\omega) \tag{10}$$

This leads to the expression

$$< \hat{C}(\gamma^A, \gamma^B, \omega) > \cong P(\omega)\, |A_m(\omega)|^2 \exp(i\, k^m(\omega)\, (s^A - s^B)) \tag{11}$$

It is therefore seen that performing the operation of eq.(6), namely

$$G(\Delta s) = \int < \hat{C}(\gamma^A, \gamma^B, \omega) > \exp(-i\, k^m(\omega)\, \Delta s)\, d\omega \tag{12}$$

yields a peak equal to the integral of $P(\omega)\, |A_m(\omega)|^2$ when $\Delta s = s^A - s^B$.

The practical implication of the result of eq.(12) is that only two digitizers and two sensors are required for data collection. Considering the 16 point grids at measurement positions A and B in the previous example, data collection in this alternate scheme consists of the recording of mean cross-correlations at each possible pair of sensor position grid points at locations A and B (i.e. all pairs consisting of one grid point from site A, the other from site B). Using a 16 point grid, this implies collecting 256 mean cross-correlations.

EXPERIMENTAL DEMONSTRATION

Leak location using spatial Fourier transform processing of cross-correlation pairs, as discussed in the preceding section, has been demonstrated experimentally. The experiment established an air leak into a vacuum by sucking air through a .028 inch hole drilled through a 3/16 inch thick aluminum plate using a vacuum hose sealed to the back side of the plate. A diagram is provided in Fig.(6). Measurement positions were chosen to detect the leak generated plate waves at distances of 4.1 cm and 15.6 cm to the right and left of the hole on the front surface of the plate. At each location, data was recorded using a broad-band pinducer in contact with the plate. Data was band-pass filtered to record from 10 kHz to 500 KHz. The pinducer has an element diameter of 1.3 mm, which is treated as a point detector at the wavelengths considered. For the bandpass and plate thickness considered, it was determined that 16 point measurement grids with 2 mm point spacing were sufficient. The 256 mean cross-correlation pairs implied by this grid configuration were collected by mechanically scanning a pair of pinducers over the 16 locations at measurement sites A and B. At each grid pair, cross-correlations were averaged until sufficiently stationary (~2000 signals), and 1024 time point segments of the mean cross-correlations were Fourier transformed in time. The data was then Fourier transformed in space, to yield the data as a function of temporal frequency ω and two spatial frequency variables γ^A, γ^B. The amplitude of the data is plotted on the plane $\gamma^A = \gamma^B$ in Fig.(7). The presence of two modes of propagation is evident. It is also evident

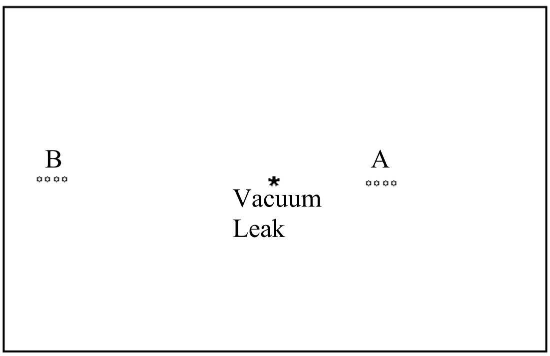

FIGURE 6. Experimental configuration for vacuum leak test.

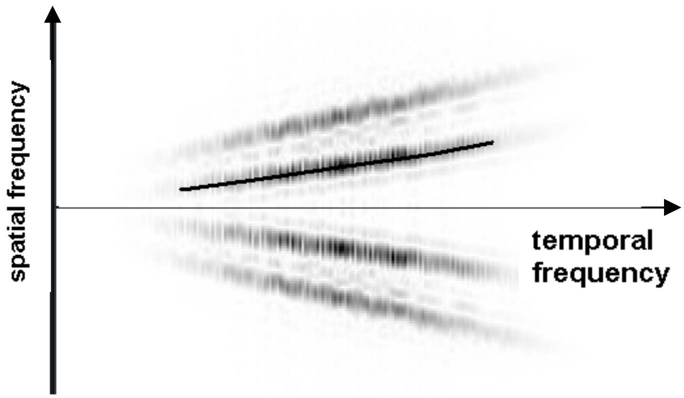

FIGURE 7. Experimental data viewed in spatial-temporal frequency plane.

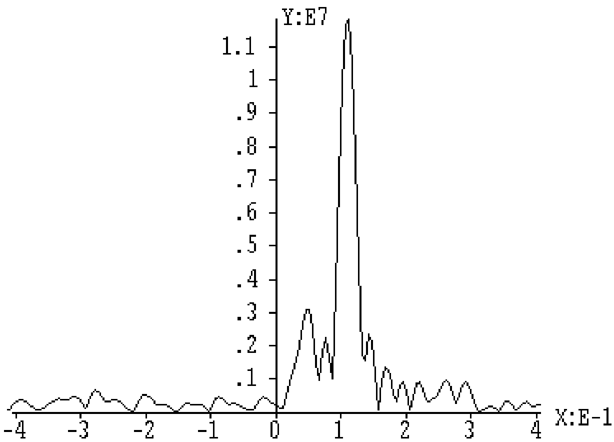

FIGURE 8. Output of the generalized cross-correlation using the isolate mode indicated in Fig.(7).

that a substantial amount of reflected energy from the plate edge is present, indicated by the signals observed in the negative spatial frequency half-plane. The prominent mode in Fig.(7) is selected for location processing. The dispersion relation k(ω) for this mode is extracted from the data by tracing the amplitude distribution, as indicated by the heavy line drawn in Fig.(7). Using this relation, the generalized cross-correlation expressed by Eq.(12) is evaluated, yielding the result plotted in Fig.(8). The leak location is unambiguously identified at Δs = 11.3 cm, indicating the difference in travel path to the leak. This is acceptably close to the actual value of 11.5 cm.

SUMMARY

It has been shown that the ill-effects of dispersive multi-mode propagation on cross-correlation based source location can compensated for by applying a spatial Fourier transform analysis of the leak signals. The analysis requires collection of data over an array of spatial points at each measurement location. The work demonstrates a procedure that will robustly account for the physics of the signal transport. However, this procedure requires a substantial increase in the amount of acquired data, and in the sophistication of the associated instrumentation. The spatial Fourier transformation of a non-repetitive signal observed at a measurement location requires the simultaneous acquisition of signals over the array of acquisition points, implying the need for an array of receivers and digitizers. It was demonstrated, however, that the dispersion compensation can be implemented using a pair of receivers and digitizers, by a procedure that records mean cross-correlation pairs while mechanically scanning the sensors over the collection grid points. It is conceivable in application that the mechanical scanning could be replaced by a receiver array, which is multiplexed to a digitizer.

The results discussed here consider the location of a leak located co-linearly between two sensors. The results of this work demonstrate that the underlying principles can be applied to signals carried by plate waves. To fully consider the source location problem in plate-like structures, the measurement configuration needs to be made fully two-dimensional. This entails the use of three measurement positions, rather than two, and the data collection grids at each measurement location must be two-dimensional, rather than linear grids as employed in the results presented here. Work is ongoing to implement these extensions, and will be reported in future proceedings.

ACKNOWLEDGEMENT

This material is based on work supported by NASA under award NAG-1-029-98.

REFERENCES

1. L.E. Rewerts, R.A. Roberts, and M.A. Clark, "Dispersion Compensation in Acoustic Emission Pipeline Leak Location," in *Review of Progress in QNDE*, 16A, eds. D.O. Thompson and D.E. Chimenti, pp. 427-434, 1997.
2. L.E. Rewerts, R.A. Roberts, and M.A. Clark, "The Role of Propagation Characteristics in Acoustic Emission Pipeline Leak Location," in *Review of Progress in QNDE*, 17A, eds. D.O. Thompson and D.E. Chimenti, pp. 501-508, 1998.